Proceedings of the 2nd Croatian Conference on Earthquake Engineering - 2CroCEE
Zagreb, Croatia - March 22 to 24, 2023

DOI: https://doi.org/10.5592/CO/2CroCEE.2023.83

STUDY OF SIMULTANEOUS INTER-STOREY DRIFT IP AND OOP LOADS ON RC FRAMES WITH AND WITHOUT INFILL WALLS AND OPENINGS BY A VARIATING ANGLE

Filip Anić[(1)], Davorin Penava[(2)], Vasilis Sarhosis[(3)], Lars Abrahamczyk[(4)]

[(1)] *Postdoctoral researcher, Josip Juraj Strossmayer University of Osijek, Faculty of Civil Engineering and Architecture Osijek, filip.anic@gfos.hr*
[(2)] *Associate professor, Josip Juraj Strossmayer University of Osijek, Faculty of Civil Engineering and Architecture Osijek, davorin.penava@gfos.hr*
[(3)] *Associate professor, University of Leeds, Faculty of Engineering and Physical Sciences, School of Civil Engineering, v.sarhosis@leeds.ac.uk*
[(4)] *Associate professor, Bauhaus-Universität Weimar, Faculty of Civil Engineering, lars.abrahamczyk@uni-weimar.de*

Abstract

Within the literature, no examples of equations were found that account for out-of-plane inter-storey drift force resistance, nor any that tested RC frames under them. Moreover, no studies were even done that combined in-plane forces. Consequently, this paper presents an equation development for estimating the resistance of RC frames containing infill walls with and without openings subjected to simultaneous IP and OoP loading. The equations were derived from data obtained from 3D high fidelity finite-element micromodels calibrated against a series of small- and large-scale experimental tests. An estimation of resistance is done by obtaining a coefficient based on the opening area and the angle of the resultant in-plane and out-of-plane load and multiplying it with the in-plane load-bearing capacity of a bare frame. The derived equation showed a good correlation with the computational data.

Keywords: in-plane, out-of-plane, simultaneous load, RC frame, infill wall, openings, resistance estimation

Abbreviations and notations

Latin based

IP	In-Plane
OoP	Out-of-Plane
V_R	Shear resistance – resultant force
$V_{R,IP,BF}$	IP Shear resistance of a BF model
k_o	Coefficient used for calculating the shear resistance of an RC frame with an infill wall and an opening
k_i	Coefficient used for calculating the shear resistance of an RC frame with an infill wall (no opening)
A_o	Area of opening
A_i	Area of infill wall

Greek-based

α	The angle of the resultant force V_R
β	The ratio of opening to infill wall area (A_o/A_i)

1. Introduction

Many modern, high-rise structures in Croatia and the rest of Europe are made of reinforced concrete (RC) frames with masonry infill walls. During an earthquake event, such structures are excited in Out-of-plane (OoP) and In-plane (IP) directions. Simply by the geometry of frame structures, its IP behaviour is always governed by inter-storey drift forces. On the other hand, the OoP ones are governed by both the inter-storey drift and inertial forces. Inertial forces are carried out by the accelerated masses of the infill wall and the inter-storey drift ones -by the movement of the rigid slab *i.e.*, the frames.

The effects of the earthquake action on frame structures were investigated in IP and OoP directions separately and in combination. The combined IP and OoP loads were considered in three ways. Firstly,

Proceedings of the 2nd Croatian Conference on Earthquake Engineering - 2CroCEE
Zagreb, Croatia - March 22 to 24, 2023

DOI: https://doi.org/10.5592/CO/2CroCEE.2023.83

previous IP damage followed by OoP load. This combination is the most prevalent in the literature. Secondly, previous OoP damage followed by IP load and thirdly simultaneous IP and OoP load. Namely, most of the research that combined the loads was done using inertial OoP load and IP load. Besides the contribution of the authors of this paper, only two were found that investigated the OoP inter-storey drift forces on the structural steel frames with masonry infill walls [1,2].

Furthermore, no equations are avaliable to consider OoP inter-storey drift forces or their combination with IP loads. All the equations within the literature are either *flexural* or *arching-action* based *i.e.*, grounded on research that used inertial force approaches [3–5].

Consequently, this paper presents a computational study and analytical model development based on the simultaneous inter-storey drift OoP and IP loads on RC frames with unreinforced masonry infill walls with and without openings.

2. Methodology

Prior to computational studies and their calibrations, a series of experimental tests were undertaken. Small-scale experiment tests were undertaken to obtain the mechanical properties of the materials involved (concrete, rebar, masonry units, mortar). Also, experimental tests were undertaken on scaled specimens of frames with and without masonry infill walls and openings. In these cases, masonry walls (shear, compression, bending) were subjected to IP [6] and OoP [7] drift-driven cyclic, quasi-static tests (Fig. Figure 1). The tested specimens included a bare frame (BF), fully infilled frame (FI), frame with centric door (CD), centric window (CW), eccentric door (ED) and eccentric window (EW) openings within the infill wall.

The frame was designed using EN1998 provisions [8] following medium ductility class specifications. The masonry infill units were locally sourced and classified as Group 2 using the EN1996 provision [9], and by the same provision, a cementitious mortar was used and classified as M5 [9].

Figure 1. Experimental tests. a) OoP bend test on masonry infill wall [10]. b) IP cyclic, quasi-static test on frames with and without masonry infill walls and openings [11]. c) IP cyclic, quasi-static test on frames with and without masonry infill walls and openings [7]

Based on the OoP wall bend experiments that were done with the load parallel and perpendicular to the bedjoints (Fig. Figure 1a) and by the IP (Fig. Figure 1b) and OoP (Fig. Figure 1c) cyclic, quasi-static tests, computational models were developed and calibrated against them [12]. The computational models were developed using a FEM 3D micromodel approach via Atena Engineering 3D [13] software with manually edited *input* files.

DOI: https://doi.org/10.5592/CO/2CroCEE.2023.83

The micromodels used the 3D solid elements to simulate concrete and masonry, 2D elements for contacts (hed- and bedjoints) and 1D truss elements for rebar (Fig. Figure 2). Nonlinear cementitious material model was used for both concrete and masonry; interface – gap elements for head- and bedjoints, and cyclic reinforcement model for rebars.

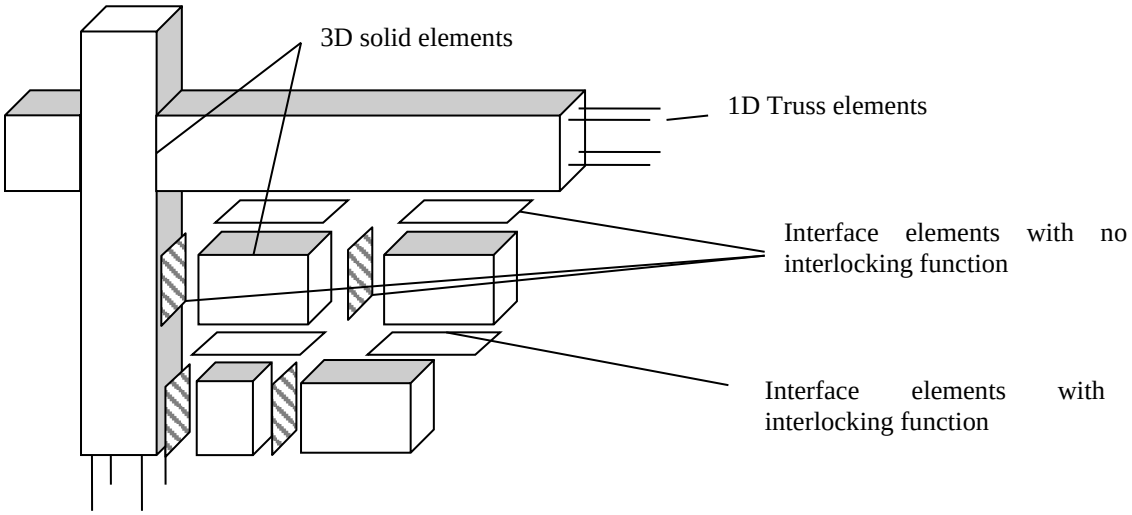

Figure 2. Parts of the 3D micromodel

The calibration process started with IP tests, followed by the OoP bend tests and finally, OoP cyclic, quasi-static tests. If there were any corrections during the process, it would be reverted to the simulation of the earlier calibrated models. Furthermore, the calibration process yielded the governing factors of each experiment.

With the calibrated models, further simulations were carried out *i.e.*, extrapolated to include simultaneous IP, OoP and gravitational load along with variating door and window opening sizes and positions.

Based on the data available in the literature, a limit of opening to infill wall area ratio was found to be $A_o/A_i \in [0.1, 0.3]$. If the ratio is below 0.1, the opening has no influence [9]; whereas if it is above 0.3, the infill wall does not [14]. Therefore, the ratios that were included in the simulations were approximately the minimum, mean, and maximum of the limits ($A_o/A_i \in \approx \{0.1,0.2,0.3\}$), an example of such variating size is visible in Figure 3 on a CW model. The dimensions of openings were chosen based on *architectural standards* that present common practices [15].

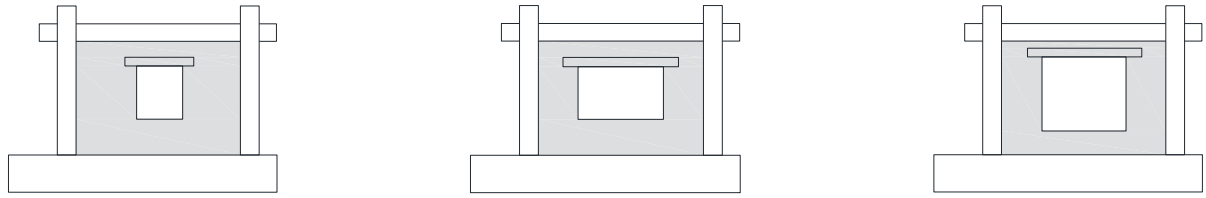

$A_o/A_i = 12.31\ \%$ $A_o/A_i = 21.54\ \%$ $A_o/A_i = 30.15\ \%$

Figure 3. Example of opening size variation on CW model

Unlike the calibrated models, the load was monotonic, *i.e.*, the pushover method. This was done since the computational time was immense, especially considering that there were more than 250 models to compute.

The simultaneous load was defined by varying the angle $\alpha \in \{0, 15, 30, 45, 60, 75, 80, 85, 90\}°$ where 0° is pure IP and 90° pure OoP load. The resultant shear load V_R is calculated by the sum of squares of IP and OoP load-bearing resistance.

Proceedings of the 2nd Croatian Conference on Earthquake Engineering - 2CroCEE
Zagreb, Croatia - March 22 to 24, 2023

DOI: https://doi.org/10.5592/CO/2CroCEE.2023.83

So, the models were further abbreviated as: $model(A_o/A_i)\{l,r\}$. Where the *model* is one of the BF, EW, etc.; *l,r* load direction in case of an eccentric opening.

3. Results and discussions

Since this paper aimed to present the equation development, only the primary outcomes of computations are presented. An example of load-bearing capacities is presented in Figure 4 in the form of a *polar plot*. The polar plot shows the values of load-bearing capacities within the polar coordinate system, where the angle of the system is also the angle of the resultant force α and the distance from the null point is the load-bearing capacity. The load-bearing capacity is expressed with its value (vertical axis) and normalised to a BF model's pure IP load-bearing capacity. The blue-filled curve is the FI's, yellow-filled BF's and cyan-filled of the referent model with openings.

The other polar plots follow the same patterns as those in Figure 4. Namely, the load-bearing capacity starts as a maximum at pure IP load ($\alpha = 0°$), and drop with the increase of α whistl finally reaching the OoP load-bearing capacity of a BF. The decline in load-bearing capacity is gradual up to 45°, while afterwards, the decline is more rapid. The reason behind it is that up to 45°, the mechanical system is frame-dominated; afterwards, it is beam-dominated. Also, with the tension introduced by bending the wall caused by OoP drift-driven load, the beneficial IP-compression strut loses its effectiveness.

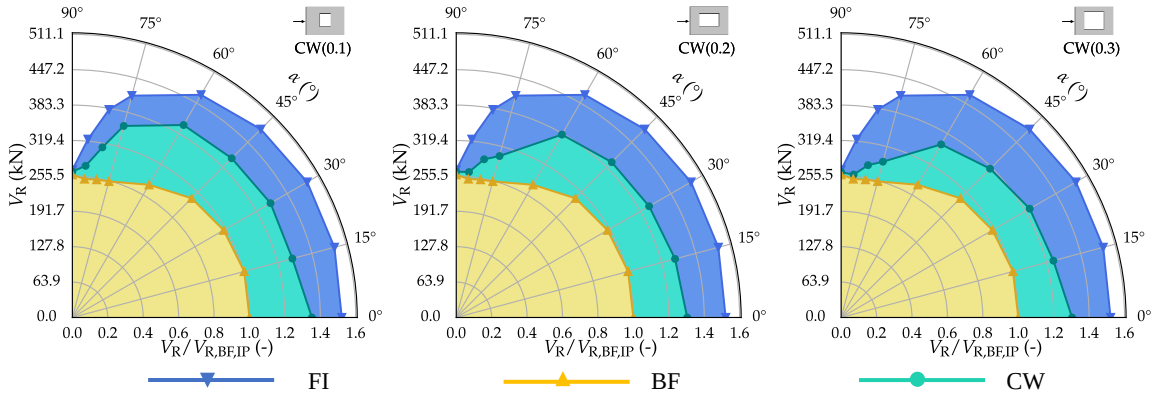

Figure 4. Example of the load-bearing capacity of CW model with different area ratios

Interaction curves were set up for one referent model *e.g.*, CW and plotted against normalized load-bearing capacity k_o, angle of the resultant force α, and the ratio of opening to infill wall area in *surface* and *contour plots* (topographical view of the surface) as visible in examples in Figure 5. Other models had similar plots, showing a mathematical pattern governing the curves.

Hence, such a mathematical pattern could be exploited to create an equation that could estimate the load-bearing capacity of an RC frame with a masonry infill wall with or without openings. The equation (Eq. 1) was arranged in a way so that the IP load-bearing capacity of a bare frame ($V_{R,BF,IP}$) is multiplied by a coefficient (k) that considers the sizes of the openings and the angle of the resultant force. Since the FI models do not have an opening, the coefficient was then divided into that those that take openings into account (k_o) and those that do not (k_i). The IP load-bearing capacity of a bare frame was chosen as a bare frame is an elementary example and IP being more researched. Such a capacity could be obtained through calculations, numerical computations or experiments.

$$V_{R,\alpha} = V_{R,BF,IP} \cdot k, \qquad k \in \{k_o, k_i\} \tag{1}$$

From the interaction curves in Figure 5, it is clear that the relation of α and normalized force is of an exponential kind, while the area ratio $\beta = A_o/A_i$ is linear. So, in order to formulate the coefficient k, first it was related to angle α forming $k(\alpha)$. Multiple equations were tested to fit the data, namely in the sphere of growth modelling (economic, natural, *etc.*). A *Monomolecular*, also known as *Brody* or *Mitscherlich* function, was implemented (Eq. 2).

Proceedings of the 2nd Croatian Conference on Earthquake Engineering - 2CroCEE
Zagreb, Croatia - March 22 to 24, 2023

DOI: https://doi.org/10.5592/CO/2CroCEE.2023.83

$$k = c_1 - \frac{c_2}{c_3}(1 - e^{-c_3 x}) \tag{2}$$

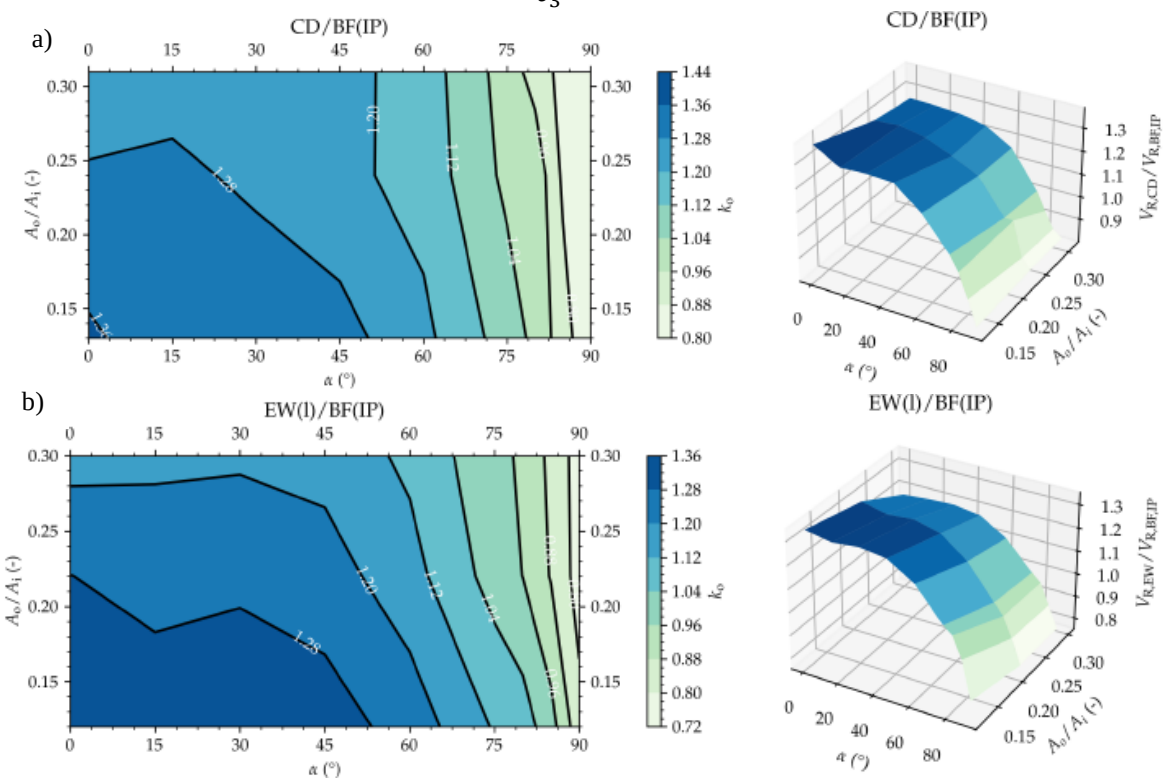

Figure 5. Example of interaction curves. a) CD model. b) EW model.

Again, the equation was then correlated to $\alpha \rightarrow k(\alpha)$ for each model of the same group by different area ratios β (*e.g.*, CW(0.1), CW(0.2), and CW(0.3)). Using a *SciPy curve fit* tool [16], the coefficients were optimised to produce the best fit with the data. So, the coefficients c_1, c_2, and c_3 were β dependable. Knowing that the β to normalized force has a linear relation, a line equation was used to calculate their governing function. Finally, with some optimisations and simplifications, the coefficient for opening (Eq. 3) and without it (Eq. 4) were formed. For the coefficient k_o That considers the openings, parameters a and b can be extracted from Table 1.

$$k_o = a + b\beta\left(1 - e^{-0.05\alpha(\beta-1)}\right) \tag{3}$$

$$k_i = 1.53 + 0.003(1 - e^{-0.085\alpha}) \tag{4}$$

$$\forall\ \alpha \in [0, 90], \beta \in [0.1, 0.3]$$

Table 1. Coefficients needed for Equation (3)

Opening		Load direction	a	b
Type	Position			
Door	Centric	/	1.29	0.071
Window	Centric	/	1.30	0.075
Door	Eccentric	Left	1.30	0.065
Door	Eccentric	Right	1.24	0.070
Window	Eccentric	Left	1.27	0.070
Window	Eccentric	Right	1.23	0.070

The equations show a good correlation with the simulation data, as visible in the examples in Figure 6. In Figure 6, the *surface* is the normalized force calculated using Equations (3,4) with the domain that

Proceedings of the 2nd Croatian Conference on Earthquake Engineering - 2CroCEE
Zagreb, Croatia - March 22 to 24, 2023

DOI: https://doi.org/10.5592/CO/2CroCEE.2023.83

covers $\alpha \in [0, 90]$ (°) and $\beta \in [0.1, 0.3]$; while the red spheres are the datapoints from micromodel computations.

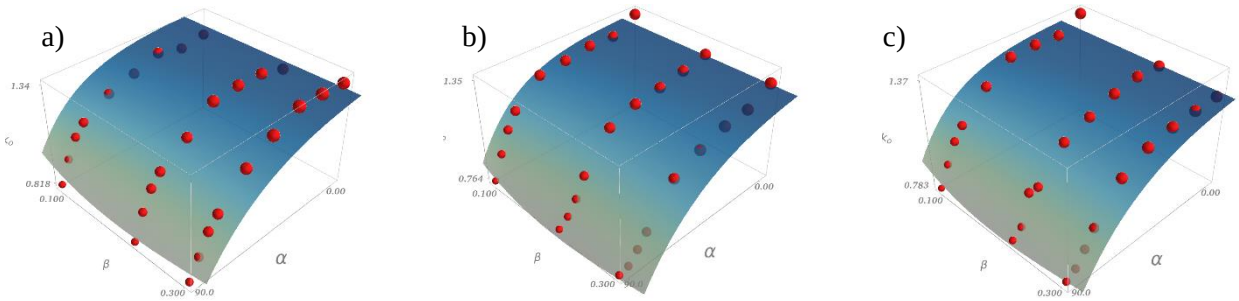

Figure 6. Data fitting results. a) CD model. b) CW model. c) ED(l) model

4. A worked example for determining the load-bearing capacity

An example of determining load-bearing capacity is described here.

Problem: Determine the load-bearing capacity of a frame with a URM infill wall and centric door opening under the angle of loading $\alpha = 45°$ (equal IP and OoP load). The IP load-bearing capacity of the frame was calculated as $V_{R,IP.BF}$ = 400 kN, and the ratio of the opening and infill wall is $A_o/A_i = \beta = 0.24$.

Solution with equations: Using Equation (3), one can obtain a more refined answer when compared to the interaction curves. Firstly, one should obtain coefficients from Table 2: a = 1.29 and b = 0.071. Then use Equation 8 with the data from the problem and Table 1.

$$\begin{aligned} k_o &= a + b\beta\left(1\text{-}e^{-0.05\alpha(\beta\text{-}1)}\right) \\ &= 1.29 + 0.071 \cdot 0.24\left(1\text{-}e^{-0.05 \cdot 45(0.24\text{-}1)}\right) \\ &\approx 1.213 \end{aligned}$$

Finally, multiply the BF's IP capacity with ko, thus obtaining the requested capacity:

$$\begin{aligned} V_{R,CD,\alpha=45} &= k_o V_{R,BF,IP} \\ &= 1.213 \cdot 400 \\ &= 485.20 \text{ kN} \end{aligned}$$

Solution with interaction curves (graphical): The process is described in Figure 7. The first one should find the appropriate interaction curve. In this case, the CD one. Then find the A_o/A_i and draw a horizontal line, in this case, red. Next, find the angle and draw the vertical line, in this case, green–coloured. The intersection of the red and green lines is the requested coefficient. A more conservative approach would read it as 1.2, more detailed would estimate it as 1.23. Finally, multiply the BF's IP capacity with the coefficient, and follow the solutions below.

Detailed approach:

$$\begin{aligned} V_{R,CD,\alpha=45} &= k_o V_{R,BF,IP} \\ &= 1.23 \cdot 400 \\ &= 492 \text{ kN} \end{aligned}$$

Conservative approach:

DOI: https://doi.org/10.5592/CO/2CroCEE.2023.83

$$= 1.2 \cdot 400$$

$$= 480 \text{ kN}$$

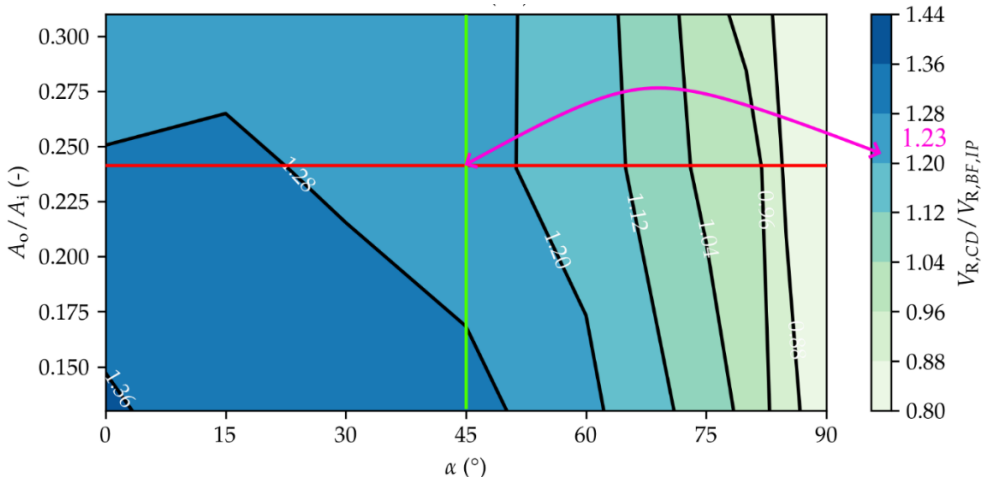

Figure 7. Determination of coefficients for the example

5. Conclusions

Using the calibrated 3D FEM micromodels, a computational campaign was conducted that included applying simultaneous IP and OoP drift-force on RC frames with and without infill walls and openings. An angle defines the simultaneous load that the resultant of IP and OoP resistance closes with the IP resistance. It was found that the greatest load-bearing capacity is with pure IP load that drops with the angle change until it reaches pure OoP load. With pure OoP load, there is no difference between the BF or other models with infill walls or openings. The decline in the capacity is gradual up to 45° when afterwards it is more rapid. Such a decline is due to a shift from the frame- to a beam-based mechanical system, and by beneficial IP compression strut losing its effectiveness caused by tension from OoP loads.

It was found that all models had similar angle-openings size-resistance interaction curves, i.e., the same mathematical pattern that accounts for the ratio of opening to infill wall area and the angle of the resultant force. Those patterns were used to derive an equation i.e., coefficients to calculate the load-bearing capacity of an RC frame with a masonry infill wall with or without openings loaded under the desired angle. The derived equation revealed a good correlation with the computational micromodel data; yet, it could not be validated against others since there is no like research with OoP drift-force approaches.

References

[1] Flanagan RD. Behavior of structural clay tile infilled frames. Tennessee, USA: 1994.
[2] Henderson R, Jones W, Burdette E, Porter M. The effect of prior out-of-plane damage on the in-plane behavior of unreinforced masonry infilled frames. Fourth DOE Nat. Phenom. Hazards Mitig. Conf., 1993, p. 18.
[3] Anić F, Penava D, Abrahamczyk L, Sarhosis V. A review of experimental and analytical studies on the out-of-plane behaviour of masonry infilled frames. Bull Earthq Eng 2020;18:2191–246. doi:10.1007/s10518-019-00771-5.
[4] Asteris PG, Antoniou ST, Sophianopoulos DS, Chrysostomou CZ. Mathematical macromodeling of infilled frames: state of the art. J Struct Eng 2011;137:1508–17. doi:10.1061/(ASCE)ST.1943-541X.0000384.
[5] Pasca M, Liberatorea L, Masiani R. Reliability of analytical models for the prediction of out-of-plane capacity of masonry infills. Struct Eng Mech n.d.;64:765–81. doi:https://doi.org/10.12989/sem.2017.64.6.765.
[6] Sigmund V, Penava D. Influence of openings, with and without confinement, on cyclic response of infilled

Proceedings of the 2nd Croatian Conference on Earthquake Engineering - 2CroCEE
Zagreb, Croatia - March 22 to 24, 2023

DOI: https://doi.org/10.5592/CO/2CroCEE.2023.83

r-c frames — an experimental study. J Earthq Eng 2014;18:113–46. doi:10.1080/13632469.2013.817362.

[7] Anić F, Penava D, Guljaš I, Sarhosis V, Abrahamczyk L. Out-of-plane cyclic response of masonry infilled RC frames: An experimental study. Eng Struct 2021;238:112258. doi:10.1016/j.engstruct.2021.112258.

[8] CEN. Eurocode 8: Design of Structures for Earthquake Resistance - Part 1: General Rules, Seismic Actions and Rules for Buildings (EN 1998-1:2004). Brussels: European Committee for Standardization; 2004.

[9] CEN. Eurocode 6: Design of masonry structures - Part 1-1: General rules for reinforced and unreinforced masonry structures (EN 1996-1-1:2005). Brussels: European Committee for Standardization; 2005.

[10] Anić F, Penava D, Varevac D, Sarhosis V. Influence of Clay Block Masonry Properties on the Out-of-Plane Behaviour of Infilled RC Frames. Teh Vjesn 2018.

[11] Penava D. Influence of openings on seismic response of masonry infilled reinforced concrete frames. 2012.

[12] Anić F, Penava D, Sarhosis V, Abrahamczyk L. Development and Calibration of a 3D Micromodel for Evaluation of Masonry Infilled RC Frame Structural Vulnerability to Earthquakes. Geosciences 2021;11:468. doi:10.3390/geosciences11110468.

[13] Cervenka Consulting. ATENA for Non-Linear Finite Element Analysis of Reinforced Concrete Structures 2015.

[14] Penava D, Sarhosis V, Kožar I, Guljaš I. Contribution of RC columns and masonry wall to the shear resistance of masonry infilled RC frames containing different in size window and door openings. Eng Struct 2018;172:105–30. doi:10.1016/j.engstruct.2018.06.007.

[15] Neufert E, Neufert P. Architects' data. 4th ed. Wiley-Blackwell; 2012.

[16] Jones E, Oliphant T, Peterson P, Others. SciPy: Open Source Scientific Tools for Python, 2001 (http://www.scipy.org/). Http://WwwScipyOrg/ 2015.